Macromolecules

ARTICLE

pubs.acs.org/Macromolecules

Oriented Morphology and Anisotropic Transport in Uniaxially Stretched Perfluorosulfonate Ionomer Membranes

Jong Keun Park,[†,§] Jing Li,[‡] Gilles M. Divoux,[†] Louis A. Madsen,[*,†] and Robert B. Moore[*,†]

[†]Department of Chemistry and Macromolecules and Interfaces Institute, Virginia Polytechnic Institute and State University, Blacksburg, Virginia 24061, United States

[‡]International Flavors and Fragrances, Union Beach, New Jersey 07735, United States

ABSTRACT: Relations between morphology and transport sensitively govern proton conductivity in perfluorsulfonate ionomers (PFSIs) and thus determine useful properties of these technologically important materials. In order to understand such relations, we have conducted a broad systematic study of H^+-form PFSI membranes over a range of uniaxial extensions and water uptakes. On the basis of small-angle X-ray scattering (SAXS) and ^2H NMR spectroscopy, uniaxial deformation induces a strong alignment of ionic domains along the stretching direction. We correlate ionic domain orientation to transport using pulsed-field-gradient ^1H NMR measurements of water diffusion coefficients along the three orthogonal membrane directions. Intriguingly, we observe that uniaxial deformation enhances water transport in one direction (parallel-to-draw direction) while reducing it in the other two directions (two orthogonal directions relative to the stretching direction). We evaluate another important transport parameter, proton conductivity, along two orthogonal in-plane directions. In agreement with water diffusion experiments, orientation of ionic channels increases proton conduction along the stretching direction while decreasing it in the perpendicular direction. These findings provide valuable fodder for optimal application of PFSI membranes as well as for the design of next generation polymer electrolyte membranes.

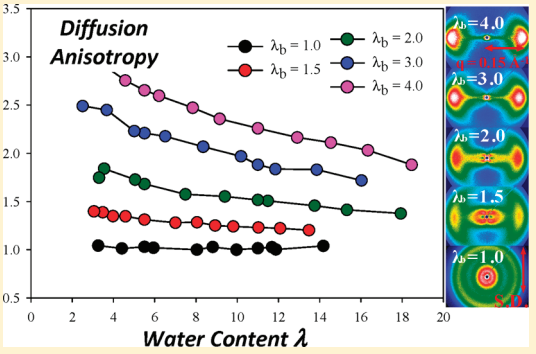

INTRODUCTION

Perfluorosulfonate ionomers (PFSIs) find fruitful application in fuel cells,[1] water electrolyzers,[2] chlor-alkali cells,[3] and soft actuators/sensors.[4,5] Their wide utilization in electrochemical/mechanical processes originates from their unique nanophase-separated morphology and excellent transport properties. The most extensively studied PFSI and the focus of the present investigation is Nafion, which is commercially available from E.I. Dupont de Nemours and Co. Nafion has the following structure:

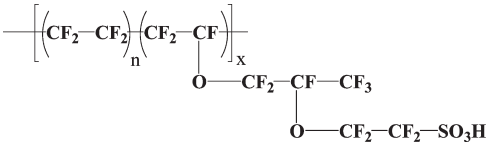

Nafion is a copolymer of tetrafluoroethylene and generally less than 15 mol % of perfluorovinylether units terminated with sulfonic acid functionalities.[1] With a sufficient length of polytetrafluoroethylene (PTFE) segments between side chains, Nafion can organize into crystalline domains generally ≤10 wt % for the 1100 equiv weight material (EW, grams of dry polymer per equivalent of sulfonic acid units). While the existence of a crystalline component in PFSI membranes is well-known, the true crystallite organization (e.g., stacked lamellae vs fringed micelles), the relationship of the crystallites to the ionic domains, and the ultimate roles of crystallinity in affecting key membrane characteristics such as water uptake, proton conductivity, and mechanical stability in this benchmark PFSI have not been fully resolved. Greater efforts, however, have been focused on the unique nanophase-separated morphology observed upon aggregation of the polar, ionic side chains within the matrix of hydrophobic PTFE. These ionic clusters, specifically their shape, spatial distribution, and connectivity, define the supramolecular organization and function of this technologically important material as an ionic conductor.

Numerous small-angle X-ray scattering (SAXS) investigations have focused on characterizing the complex, phase-separated morphology, which includes crystalline, amorphous, and ionic domains.[6−13] Specifically, the scattering maximum (often called the ionomer peak) appearing in the SAXS profile of this material at $q = 0.2$ Å^{-1} corresponds to a Bragg spacing of 50 Å.[1,6,10,14] This peak has been attributed to an interparticle scattering between the ionic aggregates dispersed in the PTFE matrix.[1] Numerous structural models have been proposed to account for the origin of the ionomer peak. The oldest but still most referenced cluster-network model of Gierke et al.[6] suggested swollen inverse micelles

Received: April 15, 2011
Revised: June 17, 2011
Published: June 28, 2011

of roughly spherical geometry that are located on a paracrystalline cubic lattice and interconnected by narrow channels of ~10 Å in size. Such models account for the ion and water transport ability exhibited by PFSIs.

While the detailed shape, size, and distribution of ionic domains require further study, hydrophilic continuous pathways must exist in order for fast proton conduction and water diffusion to occur, and recent studies have suggested elongated, locally parallel water channels.[1,15] Transport properties of PFSIs have been widely explored by various methods, such as quasi-elastic neutron scattering (QENS),[16,17] NMR,[18−21] radio tracer,[22] and impedance analysis.[18,19,23] In order to understand perfluorosulfonate ionomer membrane transport processes and probe material performance, water diffusion and proton conductivity measurements can provide complementary information. Water diffusion coefficients are often measured using pulsed-field-gradient (PFG) NMR.[19,21,24,25] For example, Zawodzinski et al.[19] showed water self-diffusion coefficients increased in an approximately linear fashion at low water content, yet began to plateau at higher water content. Several authors demonstrated that PFG NMR can also provide information on the tortuosity of the percolation pathway by measuring diffusion coefficients at various diffusion times (Δ). Zhang et al.[26] measured water diffusion coefficients as a function of Δ (ranging from 4 ms to 1 s) and found that in "as-received" extruded Nafion 117 membrane, diffusion coefficients did not depend strongly on Δ. On the contrary, the diffusion of water in solution-cast Nafion 112 had a greater dependence on diffusion times (Δ), indicative of tortuous pathways for diffusion. Recently, Ohkubo et al.[24] investigated the micrometer-scale porous structure in Nafion 117 membrane by measuring the time-dependent self-diffusion coefficients at different water content with temperatures ranging from 233 to 323 K. The results revealed that the ^{1}H self-diffusion coefficients varied with $\Delta < 2$ ms due to a micrometer-scale restricted structure and were constant above 3 ms. Li et al. directly measured the anisotropy of diffusion[21] as well as orientational order information[21,27] in Nafion 117, 112, and 212 and correlated transport anisotropy with channel alignment. Further studies by the Madsen group investigated chemically specific diffusion of ionic liquid (IL) cations and anions and water inside Nafion and found that, at least for relatively high uptakes, the activation energy for ion diffusion was unchanged for pure ILs compared to ILs absorbed into Nafion[28] and that associations among ions are drastically influenced by the charged polymer matrix.[29]

Proton transport properties of Nafion membranes are strongly influenced by the water content of the membrane. In the dry state, the Nafion membrane behaves essentially like an insulator. However, the membrane efficiently conducts once it becomes hydrated above a certain point. Early studies by Yeo[30] suggested this minimum threshold was about six water molecules per sulfonic acid site, while Pourcelly et al.[31] estimated about seven water molecules. Proton conductivity has been measured under a variety of environmental conditions, such as immersed in liquid water,[19,32] water vapor,[19,33,34] and humidified gases[35,36] and at various temperatures.[23]

On the basis of the previously proposed structural models that are often oversimplified to allow a refined analysis of the transport properties, establishing a detailed morphology−transport relationship is a challenging task. We note that the efficiency of the water/proton transport through the membrane should directly be related to how ionic percolation pathways are developed three-dimensionally within the hydrophobic PTFE matrix. In an attempt to draw detailed links between morphology and transport, here we present a systematic study of H^+-form Nafion over a range of uniaxial extensions and water uptakes. Orientation of the nanostructure has been employed to control material properties and to impart novelty. For example, we have previously demonstrated that artificial muscles based on the PFSI nanostructure altered by uniaxial orientation yielded a new anisotropic actuation response.[4] Furthermore, valuable structural/morphological information can be derived by subjecting polymeric materials to simple mechanical deformations. Several mechanical deformations such as uniaxial stretching have been employed previously to explore the complex nature of the morphology of Nafion.[9,37,38] To our knowledge, there have been no systematic studies evaluating water/proton transport behaviors in uniaxially oriented H^+-Nafion. In this study, we utilized both SAXS and ^{2}H NMR quadrupole splitting[27] to characterize the anisotropic morphology. SAXS provides anisotropy information arising from the crystalline and ionic parts of the membranes, while ^{2}H NMR of absorbed D_2O provides independent information about the hydrophilic channels.

The influence of ordered morphology on the consequent transport properties was investigated using pulsed-field-gradient (PFG) NMR to measure water diffusion coefficients in three different directions (i.e., two in-plane and one through-plane) and in-plane proton conductivities in two different directions, with respect to the uniaxial orientation direction. PFG NMR can measure transport in the absence of extensive models or concentration gradients and has no issues with contact geometry (in-plane vs through-plane) often associated with conventional proton conductivity measurements. Recently, our group has also quantitatively related these phenomena (transport and anisotropy) using the theory of diffusing liquid crystals, representing a new feature of PFSI materials.[39] Such transport-morphology relationships can provide valuable insights for predicting the performance of a membrane in a particular application and for designing new membranes.

EXPERIMENTAL SECTION

Materials. Extruded Nafion 117CS from E.I. DuPont de Nemours & Co. (1100 g/equiv, sulfonic acid form) was precleaned by refluxing in aqueous 8 M nitric acid for 2 h and then in deionized (DI) water for 1 h. These cleaned membranes were dried at 70 °C in a vacuum oven for 12 h.

Uniaxial Orientation of H^+-Nafion. Uniaxially oriented samples were prepared by cutting the precleaned and vacuum-dried H^+-Nafion membranes into dog-bone shapes (with the straight region 4 cm wide and 3 cm long) and mounting them on a specially designed drawing apparatus. This apparatus allowed drawing of H^+-Nafion membranes at 150 °C (above the α-relaxation temperature of H^+-form[40]) to extension (draw) ratios (λ_b = final length (L)/initial length (L_0)) ranging from 1 to 4 as determined by the displacement of ink marks on the samples. Temperature was increased from room temperature to 150 °C at a rate of 6 °C/min, and as soon as the temperature reached 150 °C, membranes were uniaxially deformed with a stretching rate of 10 mm/min. Once the desired draw ratio was reached, the membranes were rapidly quenched (<2 min) to room temperature to prevent thermal relaxation.[38] To prepare water-swollen samples, uniaxially oriented H^+-form membranes were then mounted in Kel-F clamps and soaked in DI water for 24 h.

Synchrotron Small-Angle X-ray Scattering (SAXS). Small-angle X-ray scattering (SAXS) was performed at Brookhaven National Laboratory on the Advanced Polymer Beamline (X27C) at the National Synchrotron Light Source. The X-ray beam wavelength was 1.366 Å, and

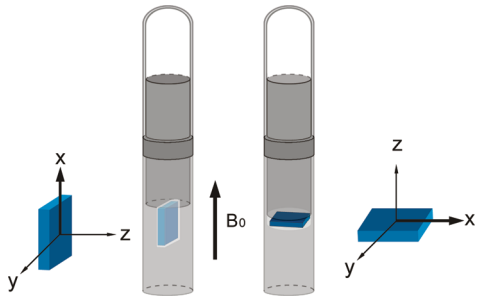

Figure 1. Sample cells for H_2O diffusion anisotropy and angle-dependent ^2H NMR experiments. For H_2O diffusion anisotropy, triple axis gradients were applied along the three membrane directions. For ^2H NMR, membrane samples were oriented with either in-plane x, y directions along the NMR magnetic field B_0 (configuration on the left) or with the through plane z direction along B_0 (configuration on the right).

the sample-to-detector distances were 1890 and 867 mm for low and medium q ranges, respectively. Two-dimensional SAXS images were recorded using a Mar CCD camera with an intensity uncertainty of ~2% and analyzed using the POLAR software developed by Stonybrook Technology and Applied Research, Inc. The relationship between pixel and the scattering vector q was determined by calibrating the scattering data with a silver behenate standard. All scattering intensities were corrected for transmission and background scatter due to air and Kapton windows and represented in arbitrary, relative intensity units as a function of q, which is a function of the scattering angle through the following relationship

$$q = \frac{4\pi}{\lambda} \sin\theta \tag{1}$$

where λ is the wavelength of X-ray beam (1.366 Å) and θ is half of the scattering angle (2θ).

^2H Quadrupolar NMR. Both ^2H NMR spectroscopy and ^1H_2O diffusion experiments (described below) were performed at 25 °C on a Bruker Avance III 9.4 T wide-bore spectrometer corresponding to a ^1H Larmor frequency of 400.13 MHz and a ^2H frequency of 61.42 MHz. A Micro5 imaging probe with triple axis gradient (maximum 298 G/cm) was used. The 8 mm double resonance coil is tunable to ^1H and ^2H. ^2H NMR was carried out using a single pulse of 10 μs ($\pi/2$ pulse = 20 μs), repetition time of 1 s (^2H T_1 varied from 50 to 250 ms), and 128 scans per spectrum. Quadrupole splittings were extracted by nonlinear least-squares fitting of each spectrum with two Lorentzian peaks using NutsPro software (Acorn NMR Inc., Livermore, CA). Controlled water uptake λ_{D_2O} and membrane sample preparation were executed as described in the next section.

^1H Pulsed Field Gradient NMR (PFG NMR). ^1H_2O diffusion experiments were performed using the PGSTE sequence[41] with δ = 2 ms and Δ = 7−50 ms. In ^1H diffusion experiments, since ^1H T_1 ranged from 80 to 350 ms, the recycle time used was 1.5 s. Four scans were coadded for each gradient step.

The NMR signal attenuation is described by the Stejskal−Tanner equation:[41]

$$I = I_0 e^{-D\gamma^2 g^2 \delta^2 (\Delta - \delta/3)} = I_0 e^{-Db} \tag{2}$$

where I is the spin−echo signal intensity, I_0 is the signal intensity using the PGSTE sequence but at zero gradient, γ is the gyromagnetic ratio of the probe nucleus (rad s^{-1} T^{-1}), δ (s) is the duration of the gradient pulse with magnitude g (T m^{-1}), D is the self-diffusion coefficient of the mobile species, Δ is the duration between the leading edges of the two gradient pulses, and b is commonly known as the Stejskal−Tanner parameter.[41] Average values of diffusion coefficients (D) were obtained from five experiments with a standard deviation of 2%.

A home-built sample cell made of Teflon and glass is depicted in Figure 1. The sample cell is pressure sealed with low dead volume (<20%) to allow membrane equilibration and minimize water evaporation. The sample cell with 8 mm o.d. fits tightly into the NMR probe insert with the aid of additional Teflon tape wrapped outside the glass tube. Diffusion anisotropy was obtained by applying pulsed-field gradients to measure ^1H_2O diffusion along three orthogonal membrane axes without repositioning the sample. We use the axis definition consistent with the membrane science convention, i.e., x is the in-plane extrusion or draw direction, y is the in-plane perpendicular direction, and z is the through-plane direction. Nafion membranes were cut into 4.5 mm × 4.5 mm pieces with one edge along the extrusion or draw direction. 6−14 pieces were stacked in exactly the same orientation to enhance NMR signal. The stack of membranes were loosely wrapped with Teflon tape and soaked in ^1H_2O for at least 1 week to obtain maximum water uptake. Water uptake expressed in wt % was determined by the measured weight gain versus the weight of the vacuum-dried membranes. The wt % of unsaturated membranes was measured by the partially swollen membrane weight and confirmed using relative NMR signal intensities. Water uptake λ_{H_2O} is defined as moles of water molecules per mole of sulfonate group. Partially swollen membranes were prepared by allowing ^1H_2O to evaporate from the membrane stack before sealing with extra Teflon tape and LDPE plastic wrap. The sealed membrane stacks were placed into the cavity of the sample cell and pressure sealed with a piston cap. An equilibration time of 3 h allowed membranes to reach steady state.

Proton Conductivity Analysis. Measurement of in-plane proton conductivity was conducted on oriented Nafion membranes using a four-point conductivity cell developed by Bekktech. To evaluate anisotropic proton conductivity, the probe was positioned onto the hydrated membranes (with a constant pressure) such that the gaps between the Pt electrodes were aligned in directions either parallel or perpendicular to the direction of uniaxial deformation. Then, the conductivity cell, loaded with a fully hydrated membrane, was stored in a humidity chamber and equilibrated at 95% RH and 80 °C for 12 h. Measurements were taken from 0.1 to 500 000 Hz using a 1255 HF frequency analyzer coupled with a 1286 electrochemical interface, both from Solatron. Data analysis was carried out using both Zplot and Zview software purchased from Scribner and Associates, Inc. The in-plane conductivity was then calculated using the definition of the resistance in terms of the bulk resistivity and the cell geometry, shown in eq 3, where ρ is the membrane resistivity ($\Omega\cdot$cm), A is the cross-sectional area perpendicular to the current flow, W is the width of the sample, d is the distance between the two reference electrodes, and T is the thickness of the film.

$$R = \frac{\rho d}{A} = \frac{\rho d}{WT} \tag{3}$$

Since conductivity is the inverse of resistivity, eq 3 can be rewritten in terms of conductivity as shown in eq 4, where σ is the conductivity (S/cm), ρ is the membrane resistivity ($\Omega\cdot$cm), and R is the membrane resistance (Ω).

$$\sigma = \frac{1}{\rho} = \frac{d}{RWT} \tag{4}$$

The membrane resistance is determined by taking the real Z-axis intercept of the complex impedance plot or the real Z value for which the phase, Φ, is equal to zero. To investigate the effects of varying water content, σ was recorded at various % RH values.

Determination of Swelling Ratio. The swelling ratios of membranes were determined by measuring the in-plane (x and y) and

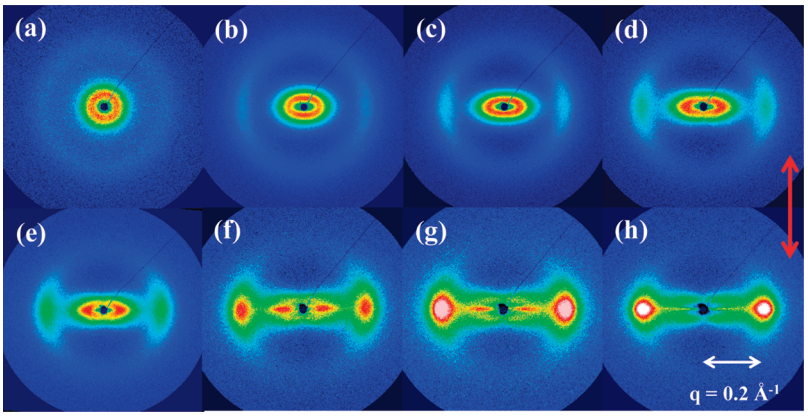

Figure 2. Two-dimensional SAXS patterns of dry H^+-form Nafion elongated to various extension ratios, $\lambda_b = L$ (final length)/L_0 (initial length). (a) $\lambda_b = 1.0$, (b) $\lambda_b = 1.25$, (c) $\lambda_b = 1.5$, (d) $\lambda_b = 1.75$, (e) $\lambda_b = 2.0$, (f) $\lambda_b = 2.5$, (g) $\lambda_b = 3.0$, and (h) $\lambda_b = 4.0$. Stretching direction is indicated with a red arrow. Samples were uniaxially stretched at 150 °C with a strain rate of 10 mm/min.

through-plane dimension (z) of the dry and hydrated membranes using a vernier caliper and a thickness gauge with 1 μm resolution, respectively. The fully hydrated membranes with various draw ratios (λ_b) were prepared in the same method as described above. These membranes were kept in a vacuum oven for 24 h at room temperature to give dry samples.

RESULTS AND DISCUSSION

Small-Angle X-ray Scattering (SAXS). The effects of uniaxial deformation on the morphology of H^+-form Nafion have been characterized by two-dimensional SAXS. For the as-received state (Figure 2a), the isotropic SAXS data show a diffuse outer ring of maximum intensity at ca. $q = 0.2$ Å^{-1}, which has been attributed to scattering from the ionic aggregates dispersed in the PTFE matrix. The intense scattering near the beam stop is associated with typical ionomer long-range heterogeneities and a contribution from PTFE-like crystalline domains. The initially isotropic intercrystalline domain peak is observed at ca. $q = 0.05$ Å^{-1} and is also shown to be sensitive to uniaxial deformation. Although beyond the scope of this investigation, it is important to point out that three recent models for the morphology of PFSIs have focused on the existence of crystallites dispersed between[42] or within[10] rodlike ionic domains or as lamellae[43] separating the ionic regions. Clearly, the proximity of the crystallites to the ionic domains differs significantly in the proposed structures, and thus fundamental research is needed to provide definitive evidence for the true semicrystalline structure in these technologically important ionomers. As the membrane is increasingly stretched up to a maximum of $\lambda_b = 4.0$, the initially isotropic scattering pattern for the ionomer peak transforms into a strongly anisotropic scattering pattern (i.e., equatorial spots) as clearly observed in Figure 2, parts f–h. At high extensions, equatorial streaking in the SAXS pattern is observed, consistent with the formation of fibrillar-like morphologies. Van der Heijden and co-workers attributed this anisotropic scattering to the alignment of elongated polymeric aggregates in the direction of uniaxial extension.[37] Recently, Rubatat and Diat suggested that the cylindrical scattering objects are simply aligned (or tilted) preferably toward the stretching direction without undergoing any significant shape change during uniaxial orientation, thus countering the idea of deformation of spherical ionic domains into ellipsoids.[12]

Because the ionomer peak is observed only along the equatorial direction for oriented samples, 1-dimensional analysis of oriented SAXS patterns can be performed at the azimuthal angle 90° (data not shown). The peak maximum q_{max} slightly shifts from 0.20 to 0.22 Å^{-1} as the draw ratio increases from $\lambda_b = 1.0$ to $\lambda_b = 1.5$. For $\lambda_b \geq 1.5$, q_{max} remains fairly constant at 0.22 Å^{-1}. This observation agrees with previous orientation studies involving Nafion membranes deformed at room temperature.[37] This indicates a decreased correlation distance along the equator as cylindrical ionic aggregates pack closer to each other.[12]

After uniaxial stretching of a dry Nafion membrane, solvent swelling is achieved by first mounting the membrane onto a Kel-F clamp and then immersing in DI water for 24 h at room temperature (RT). After removal from the clamp, no changes in the dimensions of the hydrated membranes (e.g., retraction) were observed. Without use of the Kel-F clamp, however, oriented Nafion showed some relaxation during the swelling process. Two-dimensional SAXS patterns of oriented, fully hydrated Nafion membranes shown in Figure 3 reveal that the anisotropic patterns persist even after the hydration process, indicating that no significant relaxation of the ionic aggregates is taking place. We note that in Figure 3 the sample-to-detector distance is increased to capture scattering behaviors at lower angles. This established anisotropic morphology was stable without any notable relaxation (confirmed by SAXS) even after 6 months at room temperature. It is also apparent that q_{max} shifts to lower scattering angles with solvent swelling when compared at the same draw ratios; for example, the q_{max} shifts from 0.2 Å^{-1} (dry) to 0.15 Å^{-1} (hydrated) for $\lambda_b = 4.0$. This shift to lower scattering angle is due to water enlarging the hydrophilic channels.

Figures 2 and 3 clearly indicate that the scattering intensity of the ionomer peak monotonically grows along the equatorial direction as a function of extension ratio λ_b. To quantify the degree of orientation as a function of λ_b, we have calculated the Herman's orientation function f (also known as the orientational order parameter S) from the azimuthal plots using the following equation:[44,45]

$$f = \frac{3\langle cos^2\,\chi\rangle - 1}{2} \qquad (5)$$

where χ is the azimuthal angle and $\langle \cos^2 \chi \rangle$ denotes the average of $\cos^2 \chi$. The average square of the cosine was calculated from the

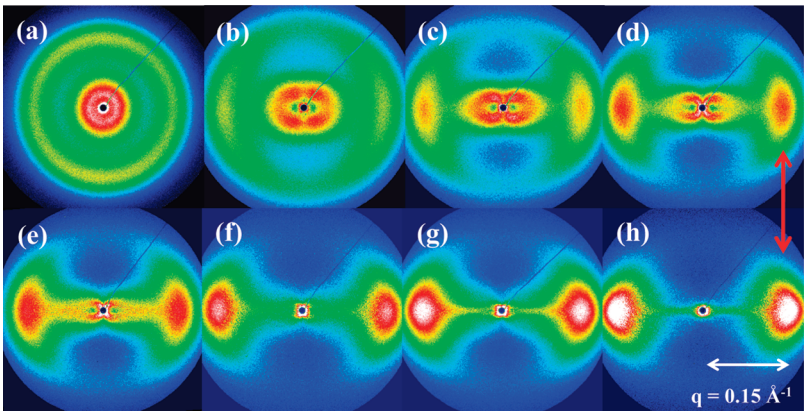

Figure 3. Two-dimensional SAXS patterns of fully hydrated H^+-form Nafion at various extension ratios, $\lambda_b = L$ (final length)/L_0 (initial length). (a) λ_b = 1.0, (b) λ_b = 1.25, (c) λ_b = 1.5, (d) λ_b = 1.75, (e) λ_b = 2.0, (f) λ_b = 2.5, (g) λ_b = 3.0, and (h) λ_b = 4.0. Stretching direction is indicated with a red arrow. Samples are hydrated after uniaxial orientation.

Table 1. Herman's Orientation Function *f* vs Extension Ratio λ_b

extension ratio (λ_b)	1.0	1.25	1.5	1.75	2.0	2.5	3.0	4.0
dried Nafion	0.08	0.52	0.56	0.62	0.64	0.70	0.72	0.76
hydrated Nafion	0.06	0.46	0.52	0.56	0.60	0.64	0.68	0.74

equation

$$\langle cos^2\,\chi\rangle = \frac{\int_{\chi_1}^{\chi_2} I(\chi)\, cos^2\,\chi\, sin\,\chi\, d\chi}{\int_{\chi_1}^{\chi_2} I(\chi)\, sin\,\chi\, d\chi} \qquad (6)$$

where $I(\chi)$ is the scattering intensity as a function of χ and the limits of integration are between χ_1 (0°) and χ_2 (180°). According to eq 5, f assumes a value of 1 for a system with perfect orientation of the scattering entities parallel to the director, −1/2 for the case where orientation of the scattering entities is perpendicular to the director, and 0 for an isotropic sample. In the case of uniaxially oriented Nafion, the director is defined as corresponding to the stretching direction. Table 1 lists f vs λ_b for both dried and hydrated Nafion membranes. It is interesting to note that there are no significant differences in f between dry and hydrated samples. This observation indicates that there is no significant structural reorganization during the swelling process. Table 1 shows that slight uniaxial deformation greatly affects f, which changes from near 0 to 0.52 at only λ_b = 1.25 for dry Nafion membrane. As λ_b increases up to 4.0, the order parameter plateaus at 0.76, indicating considerable orientation of ionic domains along the stretching direction.[37−39]

This degree of ordering is characteristic of polymers with some stable anisotropic substructure that simply rotates under uniaxial deformation, such as a liquid crystal polymer or a polymer with an anisotropic crystallite substructure. Recently, Stasiak et al.[45] investigated the strain response of styrene−isoprene−styrene (SIS) block copolymers with cylindrical (18 wt % PS) and spherical (16 wt % PS) morphologies using SAXS. Comparison of changes in orientational order parameters as a function of elongation for cylinder- and sphere-forming materials provide some basic insights into how microstructures respond to uniaxial deformation. The authors observed that the cylinder-forming morphology forms a highly ordered structure following extensional

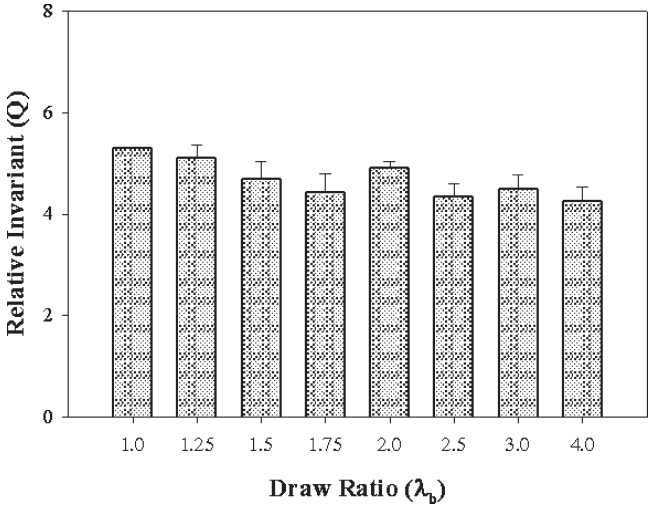

Figure 4. Scattering invariant Q extension ratio λ_b for dry, oriented membranes.

flow in the channel die and its order parameters are responsive to uniaxial deformation.[45] On the other hand, the sphere-forming material did not exhibit a well-ordered anisotropic morphology and its order parameter remained almost constant during stretching up to λ_b = 2.[45] Thus, our observations further indicate that some structural organizations of ionic domains in Nafion are more elongated (cylindrical-like) rather than spherical.[46]

In addition to changes in the spatial distribution/order of the ionic aggregates, the overall degree of phase separation, or the extent of ionic aggregation, could possibly change as well upon uniaxial deformation. In order to assess this phase separation, the scattering invariant (Q), which is a good representation of the overall degree of phase separation present in the polymer, can be calculated using

$$Q = 2\pi^2(\Delta\rho)^2 V = \int_0^\infty I(q) q^2\, dq \qquad (7)$$

where V is the volume of the scattering particles, $\Delta\rho$ is the electron density difference between scattering particles and matrix, $I(q)$ is the scattered intensity, and q is the scattering vector. Previously, Lin et al. calculated the scattering invariant Q

dx.doi.org/10.1021/ma200865p |*Macromolecules* 2011, 44, 5701–5710

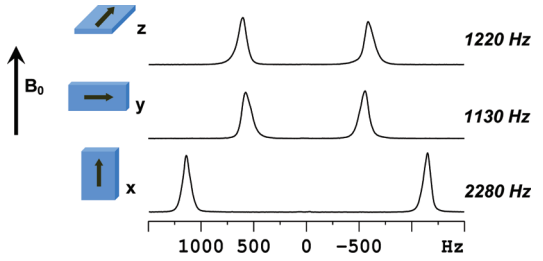

Figure 5. Representative ^{2}H NMR spectra for Nafion 117 at 10 wt % D_2O uptake (λ_{D_2O} = 5.5) and draw ratio 4.0. Blue rectangular blocks indicate different membrane directions (*x*, *y*, *z*) aligned parallel to the spectrometer B_0 field. Arrows indicate extrusion or draw direction. Quadrupole splitting values $\Delta\nu_Q$ at right result from nonlinear least-squares fits to each spectrum and have an error <±1%.

of Nafion membranes cast from various alcohol−water solutions.[47] The authors noticed that *Q* decreased as the aliphatic alcohol chain lengths increased (methanol < ethanol < 2-propanol), indicating a decrease in the phase separation between the hydrophobic and hydrophilic regions. To calculate *Q* of dry, oriented Nafion membranes, the scattering profile extracted from Figure 2 was radially integrated (over all azimuthal angles) between q = 0.1 Å^{-1} and q = 0.31 Å^{-1}, and a chart of *Q* versus λ_b is shown in Figure 4. From these data, it appears that uniaxial orientation does not induce a significant change in *Q*, indicating that the degree of overall phase separation is not affected by uniaxial deformation.

^{2}H Quadrupolar NMR. ^{2}H NMR provides information about membrane alignment through the angle-dependent quadrupole splitting $\Delta\nu_Q$. $\Delta\nu_Q$ is defined as the distance between the doublet peaks in the ^{2}H NMR spectroscopy of D_2O molecules absorbed in the membrane. A single peak is observed for an isotropic system. Peak splitting results from the anisotropic environment that the D_2O molecules sample inside the hydrophilic channels. $\Delta\nu_Q$ is a function of the anisotropy and the direction of the material alignment axis relative to the spectrometer field.[21,27]

$$\Delta\nu_Q = Q_p \rho_{int} S_{matrix} \left(\frac{3\ cos^2\ \theta - 1}{2} \right) \qquad (8)$$

where Q_p is the quadrupole coupling constant (~260 kHz) and *S* is the average order parameter of O−D bonds with respect to the alignment axis of the material. θ defines the angle between the material alignment axis and the spectrometer magnetic field B_0. S_{matrix} is the order parameter of the channel network matrix itself; ρ_{int} is the scaling factor determined by the interaction between the probe molecule and the host matrix. Here we directly determine S_{matrix} using SAXS, as reported in Table 1. This becomes a convenient method of measuring anisotropy in membranes including Nafion.[21,27,39,48]

A typical set of NMR spectra is shown in Figure 5. While the unstretched membrane shows only a small splitting due to the extrusion process, in the stretched membranes $\Delta\nu_Q$ becomes very large. Maximum splitting occurs when the membrane alignment direction is parallel to spectrometer field B_0, following eq 8. At fixed water uptake λ_{D_2O}, $\Delta\nu_Q$ increases as draw ratio increases, indicating greater alignment. $\Delta\nu_Q$ is also strongly dependent on water uptake. At lower water uptake, D_2O molecules are more strongly ordered in the channels, which can be conceptualized as the water having more interaction with the hydrophilic channel walls rather than with other water

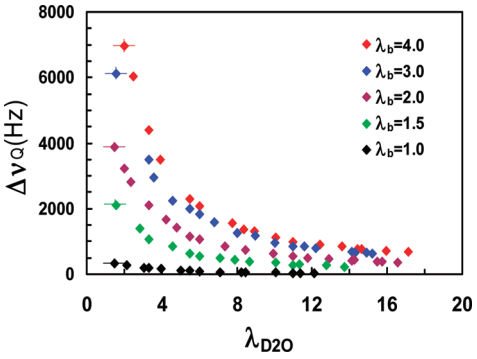

Figure 6. Quadrupole splitting $\Delta\nu_Q$ as a function of D_2O uptake in membranes at different draw ratios. Note that $\Delta\nu_Q$ is proportional to the order parameter *S* of the hydrophilic channels at a given λ but for different draw ratios. As λ_{D_2O} increases, $\Delta\nu_Q$ drops due to expansion of the channels and decreased anisotropic coupling with the D_2O.

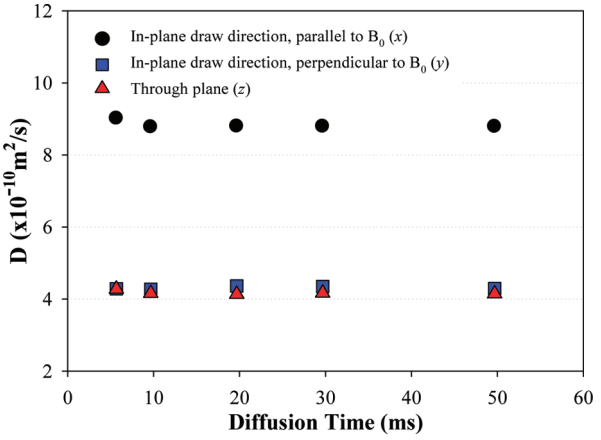

Figure 7. Water self-diffusion coefficient *D* in oriented Nafion membranes (λ_b = 4) as a function of diffusion time Δ and membrane direction (*x*, *y*, and *z*).

molecules. In other words, ρ_{int} in eq 8 is larger for smaller channels. This makes water uptake control especially important as one would like to compare material alignment using this method at identical uptake. Figure 6 shows curves of $\Delta\nu_Q$ versus water uptake at each draw ratio.

These curves contain quantitative information about ρ_{int} as a function of water uptake, and about S_{matrix} as a function of draw ratio. Our preliminary analyses show that these curves fit reasonably well to a hyperbola ($\Delta\nu_Q \propto \lambda_{D_2O}{}^{-1}$). If we assume that channel lengths are roughly fixed with swelling (see swelling data of Figure 9), we might suppose that $\lambda_{D_2O} \propto r^2$ (cross-sectional area), where *r* is the channel radius, and thus that $\Delta\nu_Q \propto r^{-2}$. This dependence requires further study in order to fully understand its significance.

Pulsed-Field-Gradient (PFG) NMR. To evaluate the effect of induced anisotropic morphology on transport properties, self-diffusion coefficients *D* of the penetrant, H_2O, were probed along three different directions: *x*, *y*, and *z*. Anisotropic water transport behaviors in PFSIs were previously reported by several authors.[21,25] Because of the weak anisotropy induced during membrane processing (i.e., melt extrusion through a die), anisotropic transport was minimal. To our knowledge, there have

dx.doi.org/10.1021/ma200865p |*Macromolecules* 2011, 44, 5701–5710

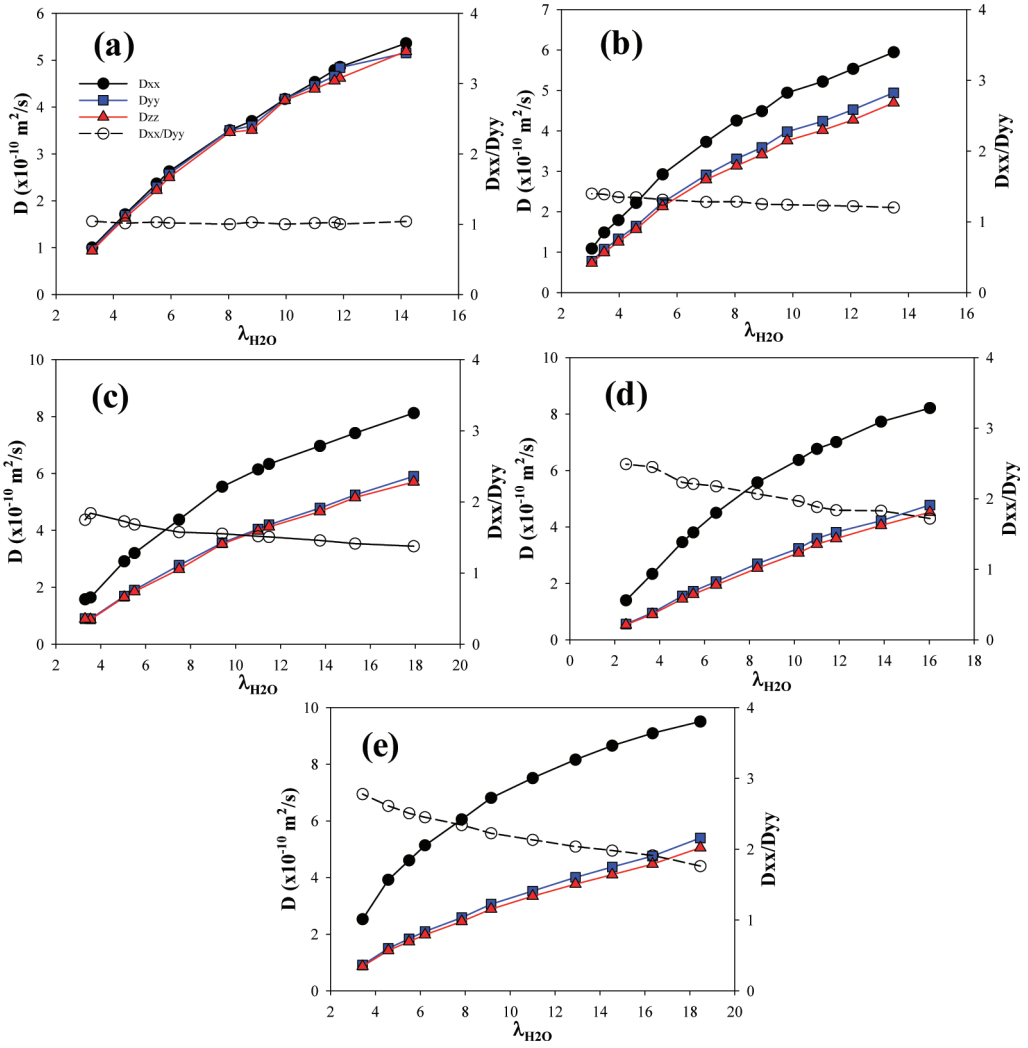

Figure 8. Water diffusion coefficient D and anisotropy D_{xx}/D_{yy} as a function of water content λ_{H_2O} in drawn Nafion with λ_b of 1.0 (a), 1.5 (b), 2.0 (c), 3.0 (d), and 4.0 (e).

been no systematic studies evaluating water transport behavior in uniaxially oriented H^+-Nafion. Figure 7 shows measured D for H_2O in oriented Nafion ($\lambda_b = 4$) as a function of the time Δ over which self-diffusion occurs in the stimulated echo pulse sequence. Diffusion time (Δ) was varied from 7 to 50 ms to look for any structural restriction that may lead to tortuous diffusion behavior in highly oriented Nafion. No significant restricted diffusion was observed previously in the range of the diffusion times employed in this study for as-received, unoriented Nafion 117.[21] However, we note that Ohkubo et al.[24] recorded a dependence of self-diffusion coefficient on Δ between 1 and 2 ms. Although our study does not include the same range of diffusion times Δ, any structural changes such as merging or elongating ionic domains during uniaxial orientation might have caused diffusive restrictions to be observed in the diffusion anisotropy at longer Δ values. Figure 7 shows that diffusion coefficients along all directions (x, y, and z) do not significantly depend on Δ. This information simply indicates that no significant structural changes on >0.5 μm scales were induced during uniaxial orientation.

The impact of uniaxial orientation on transport properties is demonstrated by comparing diffusion coefficients measured along three orthogonal membrane axes. In Figure 7, diffusion coefficients parallel to the draw direction (x) are always higher than those perpendicular-to-draw (y) and through-plane (z) directions regardless of Δ. In fact, perpendicular-to-draw and through-plane directions exhibited the same diffusion coefficients at any given Δ.

To systematically characterize how induced anisotropic morphology influences transport in Nafion, water self-diffusion coefficients D were evaluated along three different directions (D_{xx}, D_{yy}, and D_{zz}) in drawn Nafion over a range of draw ratios $\lambda_b = 1.0$ (a), 1.5 (b), 2.0 (c), 3.0 (d), and 4.0 (e) and are presented in Figure 8. In each sample, water content λ_{H_2O} is gradually decreased to investigate its effect on anisotropic transport. First, regardless of membrane orientation direction, higher water D is observed at higher λ_{H_2O}. This is not surprising since an increase in water content swells the hydrophilic ionic channels (i.e., water dynamics become more liquidlike within ionic domains with higher water content) and facilitates connectivity between the adjacent ionic domains, promoting long-range water/proton transport. In Figure 8, we also find that for all extension ratios (λ_b) D_{xx} is always greater than D_{yy} and D_{zz} at all λ_{H_2O}. Comparison to D for unoriented samples reveals that

dx.doi.org/10.1021/ma200865p |*Macromolecules* 2011, 44, 5701–5710

uniaxial deformation of Nafion membranes enhances transport in one direction (x, parallel to draw direction) while reducing it in the other two directions (y and z).[39] Faster transport along the stretching direction is thus directly related to the preferential alignment of hydrophilic channels along the draw direction as evidenced by SAXS and ^{2}H NMR. Interestingly, water transport is observed to be exactly the same along the in-plane, perpendicular-to-draw direction and through-plane direction. This observation is strong evidence for the uniaxiality of the membrane deformation process and further supports the presence of elongated hydrophilic channels that are reoriented preferentially along the stretching direction.

Figure 8 also plots the ratio of D_{xx} to D_{yy}, named the diffusion anisotropy (R_D) to clarify the differences in water D as a function of water content λ_{H_2O}. Here we have used the definition $R_D = D_{xx}/D_{yy}$ in order to make direct comparison with proton conductivity measurements described below. Notice that $R_D = 1$ for isotropic or unoriented samples and increases monotonically to 3 at high membrane elongation ($\lambda_b = 4$). Significantly, transport anisotropy is most pronounced at low λ_{H_2O}, which was also observed by Allahyarov and Taylor in their recent coarse-grained (CG) simulation efforts, although we note that the length scales probed by PFG NMR and CG simulation are quite different, micrometers as opposed to nanometers.[49] A decrease in R_D might be attributed to relaxation of oriented morphology in the presence of higher water content. However, this idea can be ruled out by considering the Herman's orientation functions for hydrated and dried samples presented in Table 1, which showed no significant difference in ionic domain ordering. Rather, this phenomenon is likely linked to an anisotropic swelling mechanism (i.e., water swelling perpendicular to the cylinder orientation axis) combined with the faster absolute D at higher λ_{H_2O}, which allows water molecules to sample a larger length scale of the inherent (anisotropic) defect structure.[50]

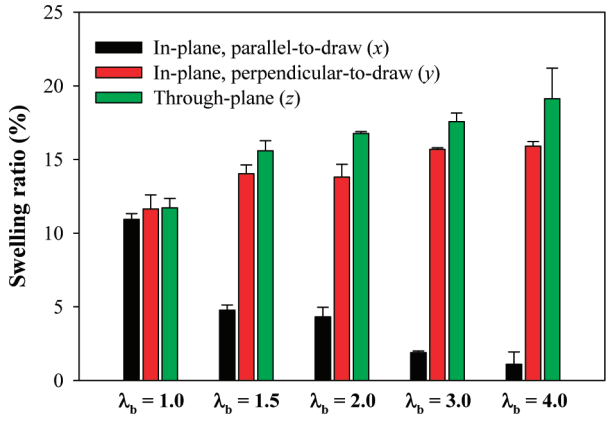

Figure 9. Anisotropic swelling behavior of uniaxially oriented Nafion membranes.

To examine the effect of uniaxial deformation on swelling behaviors, we measured dimensional changes along three different membrane axes before and after hydration (Figure 9). While unoriented Nafion undergoes essentially isotropic dimensional changes, elongated membranes show strong anisotropic swelling. Swelling through-plane (z) and in-plane perpendicular-to-draw (y) were much larger than in-plane parallel to draw (x). This anisotropic swelling is a macroscopic manifestation of the ordered microstructures in Nafion membranes.

Proton Conductivity. Proton conductivity σ often plays the role of gauging a successful ionic conductor and is measured to evaluate the viability of newly developed materials. Proton conduction in Nafion membranes is proposed to occur by three distinct mechanisms: (1) the vehicular mechanism, (2) the Grotthuss mechanism, and (3) the surface mechanism.[51] In the vehicular mechanism, proton conduction occurs with the H^+

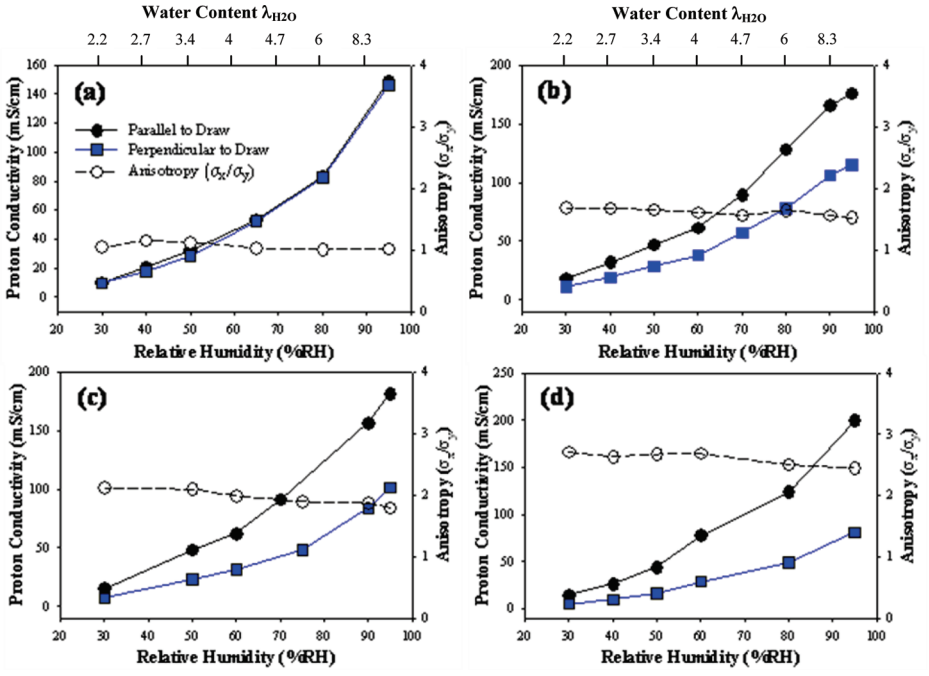

Figure 10. Proton conductivity σ and its anisotropy σ_x/σ_y as a function of relative humidity (RH) in drawn Nafion with a λ_b of 1.0 (a), 2.0 (b), 3.0 (c), and 4.0 (d). For comparison with NMR data in Figures 6 and 8, water content values are given on the upper scale, as determined by previous isotherm data on Nafion 117.[52]

localized on a mobile carrier species. Thus, the rate of diffusion of the carrier species becomes the rate-determining factor in this mechanism. In the Grotthuss mechanism, protons conduct, and thus charge transports, through "hopping" from one water molecule to another by the successive formation and breakage of hydrogen bonds. It should be pointed out that this "hopping" process is much faster than the vehicular diffusion of hydronium ions in water. Lastly, in the surface mechanism, protons conduct along the array of sulfonic acid groups, basically "hopping" from one anion moiety to another.[51]

Regardless of the detailed mechanism, proton conduction within ionomeric materials is intimately related to their morphology, specifically hydrophilic channel order/alignment. In order to understand the relationship between Nafion microstructure and σ, we measured σ along the two in-plane directions (σ_x: parallel-to-draw; σ_y: perpendicular-to-draw) on oriented Nafion membranes using a four-point conductivity cell. Figure 10 plots σ evaluated along the two directions in drawn Nafion as a function of λ_b and λ_{H_2O}. Regardless of the degree of orientation and membrane orientation direction, σ increases as a function of relative humidity (% RH), indicating a strong dependence on λ_{H_2O}. While unoriented Nafion membranes show isotropic proton conductivities, uniaxially drawn samples show a strong anisotropy, with σ_x greater than σ_y at all water contents. As observed in the diffusion results, the anisotropy of proton conductivity as a function of the draw ratio (λ_b) reflects the ordering of the hydrophilic channels as observed by SAXS and ^{2}H NMR. Figure 10 also plots the ratio of σ_x to σ_y, defined as the proton conductivity anisotropy (R_σ), to clarify the differences in proton conductivities as a function of membrane orientation direction. Here, $R_\sigma = 1$ for isotropic or unoriented samples and increases with the degree of orientation. As observed for water diffusion, the degree of anisotropy is also found to be a function of water content although the magnitude is minimal (most likely due to the narrow range of water content that can be achieved between 0 and 95% RH). Also note that, for a given draw ratio (λ_b), R_σ is quite comparable to the R_D observed at relatively low water content. This reflects the close link between these two transport parameters which are strongly influenced by the order/alignment of hydrophilic channels within Nafion membranes.

CONCLUSIONS

The effect of uniaxial orientation on the structure and transport properties of Nafion membranes was examined using a wide range of detailed analyses. SAXS experiments on dry and hydrated membranes that were uniaxially elongated above the α-relaxation temperature showed a strongly anisotropic morphology. Variably elongated membranes under a range of hydration also showed strong alignment as probed by ^{2}H NMR on absorbed D_2O. Established anisotropic morphology was shown to persist under swelling without significant relaxation. The Herman's orientation function for the ionomer peak (orientational order parameter of the polymer matrix) was strongly influenced by uniaxial deformation, which clearly supports the presence of pre-existing cylindrical (2D) rather than spherical (1D) morphology in the ionomer microstructure. Related measurements combined with theory developed for oriented liquid crystals have successfully supported this view as well.[39]

Comparison of the water diffusion coefficients between unoriented and oriented samples reveals that uniaxial deformation of Nafion membranes enhances transport in one direction (parallel-to-draw direction) and reduces it in the other two directions (two orthogonal directions relative to the stretching direction). In agreement with water diffusion experiments and SAXS results, proton conductivities evaluated along two different in-plane directions, parallel-to-draw (σ_x) and perpendicular-to-draw (σ_x), showed that ordering of the hydrophilic channels significantly increases proton conduction. We are undertaking further studies to quantitatively measure and understand the relationships between channel dimensions, domain structure, anisotropy, and mobile species transport.

AUTHOR INFORMATION

Corresponding Authors

*E-mail: lmadsen@vt.edu and rbmoore3@vt.edu.

Present Addresses

[§]The Dow Chemical Company, Marlborough, MA 01752.

ACKNOWLEDGMENT

Support for this work was provided by the National Science Foundation CMMI-0707364, CBET-0756439, and DMR-0844933. This material is further based upon work supported in part by the U.S. Army Research Office under Grant W911NF-07-1-0452 Ionic Liquids in Electro-Active Devices (ILEAD) MURI. Use of the National Synchrotron Light Source, Brookhaven National Laboratory, was supported by the U.S. Department of Energy, Office of Science, Office of Basic Energy Sciences, under Contract DE-AC02-98CH10886.

REFERENCES

(1) Mauritz, K. A.; Moore, R. B. *Chem. Rev.* **2004**, *104*, 4535–4585.
(2) Yeo, R. S.; McBreen, J.; Kissel, G.; Kulesa, F.; Srinivasan, S. *J. Appl. Electrochem.* **1980**, *10*, 741–747.
(3) Grot, W. *Chem. Ing. Tech.* **1978**, *50*, 299–301.
(4) Park, J. K.; Moore, R. B. *ACS Appl. Mater. Interfaces* **2009**, *1*, 697–702.
(5) Bennett, M. D.; Leo, D. J. *Sens. Actuators, A* **2004**, *115*, 79–90.
(6) Gierke, T. D.; Munn, G. E.; Wilson, F. C. *J. Polym. Sci., Polym. Phys. Ed.* **1981**, *19*, 1687–1704.
(7) Fujimura, M.; Hashimoto, T.; Kawai, H. *Macromolecules* **1982**, *15*, 136–144.
(8) Elliott, J. A.; Hanna, S.; Elliott, A. M. S.; Cooley, G. E. *Macromolecules* **2000**, *33*, 4161–4171.
(9) Londono, J. D.; Davidson, R. V.; Mazur, S. *Polym. Mater.: Sci. Eng.* **2001**, *85*, 23.
(10) Rubatat, L.; Rollet, A. L.; Gebel, G.; Diat, O. *Macromolecules* **2002**, *35*, 4050–4055.
(11) Page, K. A.; Cable, K. M.; Moore, R. B. *Macromolecules* **2005**, *38*, 6472–6484.
(12) Rubatat, L.; Diat, O. *Macromolecules* **2007**, *40*, 9455–9462.
(13) Haubold, H.-G.; Vad, T.; Jungbluth, H.; Hiller, P. *Electrochim. Acta* **2001**, *46*, 1559–1563.
(14) Page, K. A.; Park, J. K.; Moore, R. B.; Sakai, V. G. *Macromolecules* **2009**, *42*, 2729–2736.
(15) Schmidt-Rohr, K.; Chen, Q. *Nature Mater.* **2008**, *7*, 75–83.
(16) Pivovar, A. M.; Pivovar, B. S. *J. Phys. Chem. B* **2005**, *109*, 785–793.
(17) Perrin, J.-C.; Lyonnard, S.; Volino, F. *J. Phys. Chem. C* **2007**, *111*, 3393–3404.
(18) Saito, M.; Arimura, N.; Hayamizu, K.; Okada, T. *J. Phys. Chem. B* **2004**, *108*, 16064–16070.

(19) Zawodzinski, T. A., Jr.; Neeman, M.; Sillerud, L. O.; Gottesfeld, S. *J. Phys. Chem.* **1991**, *95*, 6040–6044.
(20) Ma, S.; Siroma, Z.; Tanaka, H. *J. Electrochem. Soc.* **2006**, *153*, A2274–A2281.
(21) Li, J.; Wilmsmeyer, K. G.; Madsen, L. A. *Macromolecules* **2009**, *42*, 255–262.
(22) Rollet, A.-L.; Jardat, M.; Dufreche, J.-F.; Turq, P.; Canet, D. *J. Mol. Liq.* **2001**, *92*, 53–65.
(23) Lee, C. H.; Park, H. B.; Lee, Y. M.; Lee, R. D. *Ind. Eng. Chem. Res.* **2005**, *44*, 7617–7626.
(24) Ohkubo, T.; Kidena, K.; Ohira, A. *Macromolecules* **2008**, *41*, 8688–8693.
(25) Kidena, K. *J. Membr. Sci.* **2008**, *323*, 201–206.
(26) Zhang, J.; Giotto, M. V.; Wen, W.-Y.; Jones, A. A. *J. Membr. Sci.* **2006**, *269*, 118–125.
(27) Li, J.; Wilmsmeyer, K. G.; Madsen, L. A. *Macromolecules* **2008**, *41*, 4555–4557.
(28) Li, J.; Wilmsmeyer, K. G.; Hou, J. B.; Madsen, L. A. *Soft Matter* **2009**, *5*, 2596–2602.
(29) Hou, J. B.; Zhang, Z.; Madsen, L. A. *J. Phys. Chem. B* **2011**, *115*, 4576–4582.
(30) Yeo, R. S. *J. Electrochem. Soc.* **1983**, *130*, 533–538.
(31) Pourcelly, G.; Oikonomou, A.; Gavach, C. *J. Electroanal. Chem.* **1990**, *287*, 43–59.
(32) Edmondson, C. A.; Stallworth, P. E.; Wintersgill, M. C.; Fontanella, J. J.; Dai, Y.; Greenbaum, S. G. *Electrochim. Acta* **1998**, *43*, 1295–1299.
(33) Rieke, P. C.; Vanderborgh, N. E. *J. Membr. Sci.* **1987**, *32*, 313–328.
(34) Nouel, K. M.; Fedkiw, P. S. *Electrochim. Acta* **1998**, *43*, 2381–2387.
(35) Wakizoe, M.; Velev, O. A.; Srinivasan, S. *Electrochim. Acta* **1995**, *40*, 335–344.
(36) Buchi, F. N.; Scherer, G. G. *J. Electroanal. Chem.* **1996**, *404*, 37–43.
(37) Van der Heijden, P. C.; Rubatat, L.; Diat, O. *Macromolecules* **2004**, *37*, 5327–5336.
(38) Page, K. A.; Landis, F. A.; Phillips, A. K.; Moore, R. B. *Macromolecules* **2006**, *39*, 3939–3946.
(39) Li, J.; Park, J. K.; Moore, R. B.; Madsen, L. A. *Nature Mater.* **2011**, *10*, 507–511.
(40) Osborn, S. J.; Hassan, M. K.; Divoux, G. M.; Rhoades, D. W.; Mauritz, K. A.; Moore, R. B. *Macromolecules* **2007**, *40*, 3886–3890.
(41) Stejskal, E. O.; Tanner, J. E. *J. Chem. Phys.* **1965**, *42*, 288–292.
(42) Kim, M.-H.; Glinka, C. J.; Grot, S. A.; Grot, W. G. *Macromolecules* **2006**, *39*, 4775–4787.
(43) Litt, M. H. *Polym. Prepr.* **1997**, *38*, 80–81.
(44) Wilkes, G. L.; Stein, R. S. In *Structure and Properties of Oriented Polymers*; Ward, I. M., Ed.; Chapman & Hall: London, 1997; pp 44−135.
(45) Stasiak, J.; Squires, A. M.; Castelletto, V.; Hamley, I. W.; Moggridge, G. D. *Macromolecules* **2009**, *42*, 5256–5265.
(46) Bass, M.; Berman, A.; Singh, A.; Konovalov, O.; Freger, V. *J. Phys. Chem. B* **2010**, *114*, 3784–3790.
(47) Lin, H.-L.; Yu, T. L.; Huang, C.-H.; Lin, T.-L. *J. Polym. Sci., Polym. Phys.* **2005**, *43*, 3044–3057.
(48) Rankothge, M.; Haryadi; Moran, G.; Hook, J.; Gorkom, L. V. *Solid State Ionics* **1994**, *67*, 241–248.
(49) Allahyarov, E.; Taylor, P. L. *J. Phys. Chem. B* **2009**, *113*, 610–617.
(50) Hou, J. B.; Li, J.; Madsen, L. A. *Macromolecules* **2010**, *43*, 347–353.
(51) Kreuer, K.-D. *Chem. Mater.* **1996**, *8*, 610–641.
(52) Zawodzinski, T. A.; Derouin, C.; Radzinski, S.; Sherman, R. J.; Smith, V. T.; Springer, T. E.; Gottesfeld, S. *J. Electrochem. Soc.* **1993**, *140*, 1041–1047.